



# Ultrasonication-assisted synthesis of gold nanoparticles decorated ultrathin graphitic carbon nitride nanosheets as a highly efficient electrocatalyst for sensitive analysis of caffeic acid in food samples

Manikandan Ramalingam<sup>1</sup> · Thangavelu Kokulnathan<sup>2</sup> · Pei-Chien Tsai<sup>1</sup> · Mariadhas Valan Arasu<sup>3</sup> · Naif Abdullah Al-Dhabi<sup>3</sup> · Karthikeyan Prakasham<sup>4</sup> · Vinoth Kumar Ponnusamy<sup>1,4,5,6,7</sup>

Received: 26 January 2021 / Accepted: 24 May 2021 / Published online: 7 July 2021  
© King Abdulaziz City for Science and Technology 2021

## Abstract

This study demonstrates a facile ultrasonication-assisted synthesis of gold nanoparticles (AuNPs) decorated ultrathin graphitic carbon nitride nanosheets ( $g\text{-C}_3\text{N}_4$ ) composite as an efficient electrocatalyst material. The as-prepared  $g\text{-C}_3\text{N}_4/\text{AuNPs}$  composite material's structural morphology was characterized using an X-ray diffractometer, field-emission scanning electron microscopy, and transmission electron microscopy. The prepared nanomaterial was applied to fabricate  $g\text{-C}_3\text{N}_4/\text{AuNPs}$  composite modified screen-printed carbon electrode (SPE) sensor for the sensitive electrochemical detection of caffeic acid (CA) in various food samples. The electrocatalytic properties and interfacial electron movement behavior of the  $g\text{-C}_3\text{N}_4/\text{AuNPs}/\text{SPE}$  was examined using electrochemical techniques, including cyclic voltammetry, chronoamperometry, differential pulse voltammetry (DPV), and electrochemical impedance spectroscopy. Under the optimized experimental conditions,  $g\text{-C}_3\text{N}_4/\text{AuNPs}/\text{SPE}$  exhibited rapid response and sensitive detection of CA in both amperometric and voltammetric techniques. Excellent linear ranges and detection limits were achieved between the CA's concentration ranging from 0.5 to 155 nM for DPV with the detection limit (LOD) of 0.1 nM and 2.5–1025 nM CA for amperometric technique with LOD of 0.5 nM. The  $g\text{-C}_3\text{N}_4/\text{AuNPs}/\text{SPE}$  sensor was successfully applied to quantify the amount of CA in various food samples, and the obtained results were promising over conventional and recently reported methods. Thus, the developed sensor can be applied in routine food quality control and food analysis laboratories for quick and sensitive quantification of CA in foods.

**Keywords** Graphitic carbon nitride nanosheets · Gold nanoparticles · Sonochemical method · Caffeic acid · Modified electrode · Food samples

## Introduction

Caffeic acid (3,4-dihydroxycinnamic acid) is an antioxidant, antineoplastic, and anti-inflammatory compound that widely occurs in various vegetables and fruits. Therefore, CA is

commonly added in multiple alcoholic and non-alcoholic beverage products. Monitoring and quantification of CA is a vital interest in food industries during food processing and production of various beverage products and nutraceutical and dietary supplements. Several recent studies have

✉ Vinoth Kumar Ponnusamy  
kumar@kmu.edu.tw

<sup>1</sup> Nano and Green Analytical Lab, Department of Medicinal and Applied Chemistry, College of Life Sciences, Kaohsiung Medical University, No. 100, Shiquan 1st Road, Sanmin District, Kaohsiung City 807, Taiwan

<sup>2</sup> Institute of Electro-Optical Engineering, National Taipei University of Technology, Taipei City, Taiwan

<sup>3</sup> Department of Botany and Microbiology, College of Science, King Saud University, P.O. Box 2455, Riyadh 11451, Saudi Arabia

<sup>4</sup> Research Center for Environmental Medicine, College of Medicine, Kaohsiung Medical University, Kaohsiung 807, Taiwan

<sup>5</sup> Department of Medical Research, Kaohsiung Medical University Hospital (KMUH), Kaohsiung City 807, Taiwan

<sup>6</sup> Department of Chemistry, National Sun Yat-Sen University (NSYSU), Kaohsiung City 807, Taiwan

<sup>7</sup> Ph.D. Program of Aquatic Science and Technology, College of Hydrosphere Science, National Kaohsiung University of Science and Technology (NKUST), Kaohsiung City 807, Taiwan

reported CA's toxicity at high dose exposure, especially, CA causes oxidative damage of lymphocytes in the human body. Also, CA shows toxicity linked with radiation and chemotherapy (Prasad et al. 2009). Therefore, it is vital to determine the CA concentration in food products as a quality control procedure in food industries.

Several analytical techniques have been demonstrated to analyze and monitor the CA, including spectroscopic and chromatographic methods (Wang et al. 2004), and electrochemical techniques (Fan et al. 2017; Leite, Santos and Kubota 2014). Compared with other analytical methods, the voltammetry techniques provide rapid and sensitive results without using any sample pretreatment and preparation steps. It is also easy to operate the instrument, and even on-site sample analysis is possible. Notably, there are no reports for highly sensitive sensors for the analysis of CA in food samples. Therefore, it is essential to develop a sensitive sensor to monitor CA in different food samples.

Recently, semiconducting nanomaterials such as transition metal oxides, boron nitrides, and graphitic carbon nitrides (g-C<sub>3</sub>N<sub>4</sub>) exhibit different morphologies, including nanosheets, nanohybrids, and nanotubes that have captivated enormous attention among electrochemical researchers due to exemplary catalytic, optical, and electrical properties (Lee et al. 2007; Li et al. 2019; Zhang et al. 2016). These nanomaterials are potentially applied in various applications such as gas sensing (Han et al. 2019a, b), optical sensors (Sikarwar & Yadav 2015), and other sensing devices (Ding et al. 2018; Karthick Kannan et al. 2019). The g-C<sub>3</sub>N<sub>4</sub> is a semiconducting (two-dimensional, 2D) nanomaterial that has been synthesized via several preparation methods, including hydrothermal, pyrolysis, and chemical vapor deposition methods. The bulk g-C<sub>3</sub>N<sub>4</sub> has a stack layered flaky structure and it has considerable electrical and optical properties that have been reported recently (Chen et al. 2019; Safaei et al. 2018a, b; Zhang et al. 2019; Zhao et al. 2019). The nitrogen-rich g-C<sub>3</sub>N<sub>4</sub> nanosheets possess a durable mechanical property, an excellent electrical nature, and thermal and chemical stabilities (Lu et al. 2015). g-C<sub>3</sub>N<sub>4</sub> is utilized for various electrochemical purposes such as a metal-free electrocatalyst for different reduction and oxidation reactions (Cheng 2019; Samanta 2019), organic catalysis, and photochemical reactions (Ghafuri 2019; Luo et al. 2019). The primary purpose of using the g-C<sub>3</sub>N<sub>4</sub> nanosheets is to enhance the transport charge and combine the charge carriers' feasibility. Hence, these materials are used as a potential electrocatalyst for different electrochemical reactions (Han et al. 2019a, b). Thus, the g-C<sub>3</sub>N<sub>4</sub> nanosheets are widely used in catalysis and energy storage devices and are excellent suitable materials in the area of electrochemical sensing platforms (Safaei et al. 2018a, b).

Recently, Fan et al. have reported the ZnO coated exfoliated graphitic carbon nitride nanosheets composite to enhance the adsorption and detection of hydrogen peroxide (Tian 2017) due to the synergetic effect of conductivity and catalytic activity. Liu et al. reported a flower-like Co<sub>3</sub>O<sub>4</sub>/g-C<sub>3</sub>N<sub>4</sub> nanocomposite as an efficient electrocatalyst towards hydrazine sensing (Dai et al. 2017). Lu et al. presented the poly(di-allyl-di-methyl-ammonium chloride)/g-C<sub>3</sub>N<sub>4</sub>/ionic liquid composite to detect tetrabromobisphenol A (Zhao et al. 2017). Wang et al. reported that g-C<sub>3</sub>N<sub>4</sub>/α-Fe<sub>2</sub>O<sub>3</sub> nanocomposite could be used for energy storage and as a glucose sensor (Liu 2016). Zhao et al. reported 3D g-C<sub>3</sub>N<sub>4</sub>/MWCNTs for high, efficient electrochemical simultaneous sensing of dopamine, uric acid, and tryptophan (Wang et al. 2016). Kim et al. reported cylindrical spongy polypyrrole doped protonated g-C<sub>3</sub>N<sub>4</sub> nanocomposite to analyze cholesterol (Shrestha 2017).

In this work, gold nanoparticles (AuNPs) decorated ultrathin graphitic carbon nitride nanosheet (g-C<sub>3</sub>N<sub>4</sub>) composite material was developed using a simple sonochemical technique. The as-prepared g-C<sub>3</sub>N<sub>4</sub>/AuNPs composite was utilized to fabricate a modified screen-printed carbon electrode (SPE) for the sensitive electrochemical analysis of CA in various food samples. Different experimental parameters affecting the electrochemical detection of CA were thoroughly optimized and applied to the analysis of the real samples.

## Experimental methods

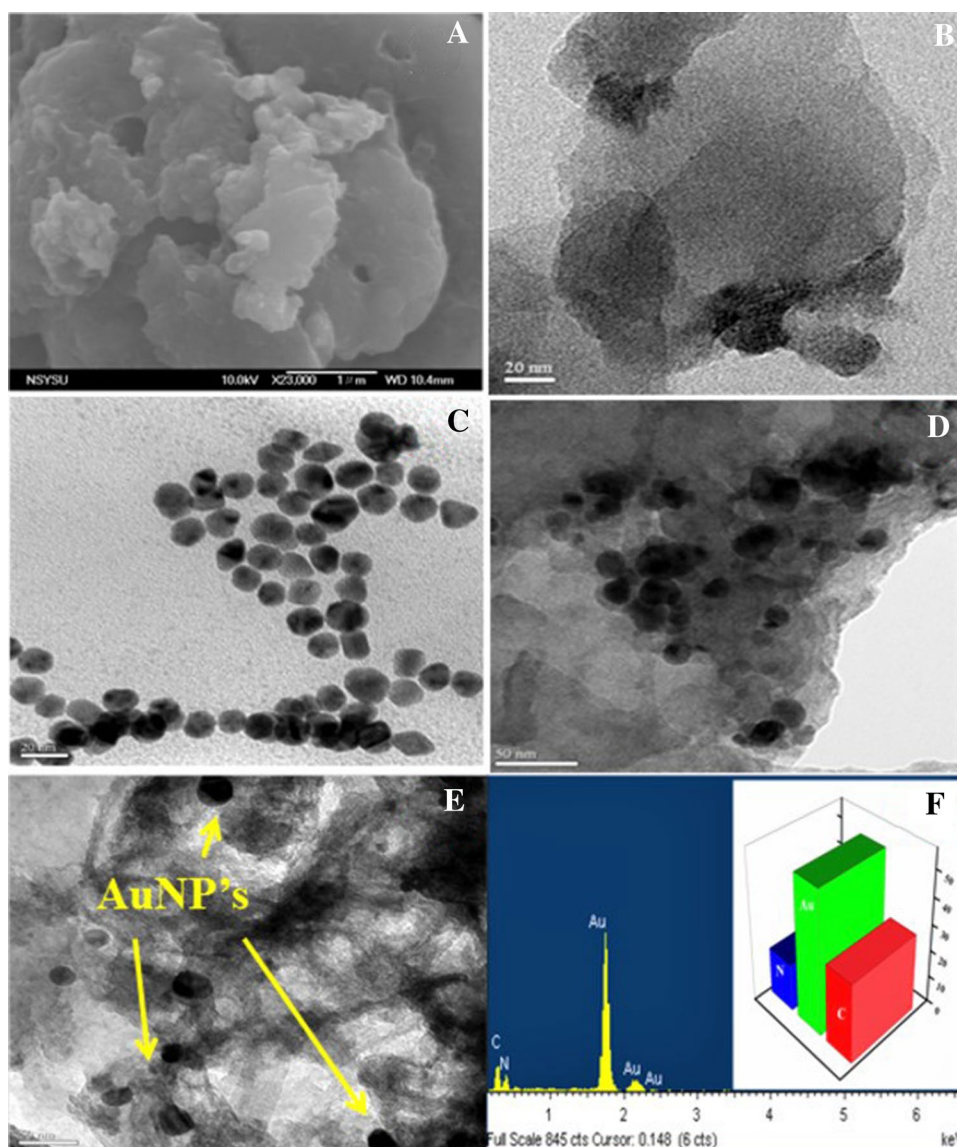
### Chemicals and reagents

Auric chloride (99.9% of HAuCl<sub>4</sub>, A.R grade) and caffeic acid (CA, 99.5%, HPLC grade) were obtained from Sigma Aldrich chemicals (USA). AR grade melamine, sodium acetate, acetic acid, disodium hydrogen phosphate, dihydrogen sodium phosphate, and potassium chloride were purchased from Xilong Scientific Co. Ltd., (Shanghai, China). K<sub>4</sub>[Fe(CN)<sub>6</sub>], and K<sub>3</sub>[Fe(CN)<sub>6</sub>] were purchased from Showa chemicals Co. Ltd., (Japan). Sulphuric acid was purchased from Fisher scientific company (UK). CA stock solution (5 × 10<sup>-5</sup> M) was prepared using ultrapure water (18.2 MΩ cm<sup>-1</sup>) (Uniss ultrapure water system, Taiwan). Singledisk (5 mm electrode surface) carbon screen-printed electrode (SPE) was obtained from Zensor Corporation (Taiwan).

### Instrumentation

All the electrochemical experiments were carried out using the electrochemical workstation (CHI 210D, CH Instruments, USA). A three-electrode system was utilized for the entire analysis (Ag/AgCl electrode as a reference

**Fig. 1** **A** FE-SEM images of bulk g-C<sub>3</sub>N<sub>4</sub>, **B** TEM images of g-C<sub>3</sub>N<sub>4</sub> nanosheets, **C** TEM images of AuNPs, **D** & **E** ultrathin g-C<sub>3</sub>N<sub>4</sub>/AuNPs nanocomposite, and **F** corresponding EDS spectrum of g-C<sub>3</sub>N<sub>4</sub>/AuNPs nanocomposite



electrode, platinum wire electrode as an auxiliary electrode and SPE was used as a working electrode). The pH of the solutions was analyzed using a SP-2100 Sutex pH meter (Taiwan). Field-emission scanning electron microscopic (FE-SEM) images were observed using Jeol FE-SEM (JSM 6500F, Japan). Powder X-ray diffraction (XRD) analysis was carried out using Bruker D8 XRD advanced model (Germany).

### Synthesis of ultrathin g-C<sub>3</sub>N<sub>4</sub>

5 g of melamine was placed in a crucible and heated at 550 °C for 2 h in a muffle furnace under a nitrogen atmosphere. The obtained yellow color solid residue was transferred into a beaker to attain room temperature. Later the yellow solid substance was transferred into 200 mL of 5%

HCl solution. Then, the mixture solution was ultrasonicated for 3 h at room temperature (Ramalingam et al. 2019). The well-dispersed mixture was centrifuged at 5000 rpm for 10 min, and the obtained residue product was dried in a hot-air oven at 60 °C for 24 h to achieve dull-white colored ultrathin g-C<sub>3</sub>N<sub>4</sub> nanosheet powder, and the obtained material was used for further studies.

### Synthesis of gold nanoparticles

Gold nanoparticles (AuNPs) were prepared based on the earlier report (Prabhu 2011) with minor modifications. 38.8 mM of sodium citrate solution was added dropwise into 0.01% of HAuCl<sub>4</sub> solution under stirring at 105 °C. Then, the mixture was boiled for 15 min under stirring to achieve citrate-capped AuNPs.

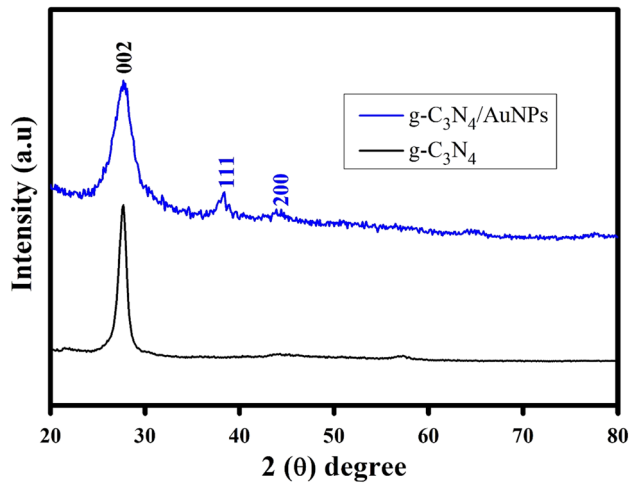


**Fig. 2** XRD of  $g\text{-C}_3\text{N}_4$  and  $g\text{-C}_3\text{N}_4/\text{AuNPs}$  nanocomposite

### Ultrasonication-assisted preparation of $g\text{-C}_3\text{N}_4/\text{AuNPs}$ composite

10 mg of ultrathin  $g\text{-C}_3\text{N}_4$  nanosheets was added into 2.7 mL of ethanol and ultrasonicated for 30 min followed by the subsequent addition of 300  $\mu\text{L}$  of the as-prepared citrate-capped AuNPs into the above suspension under ultrasonication for 3 h to obtain the AuNPs decorated on the ultrathin  $g\text{-C}_3\text{N}_4$  composite material.

### Fabrication of ultrathin $g\text{-C}_3\text{N}_4/\text{AuNPs}/\text{SPE}$ sensor

SPE was washed using ultrapure water and ethanol, and the cleaned SPE was dried at room temperature for 30 min.

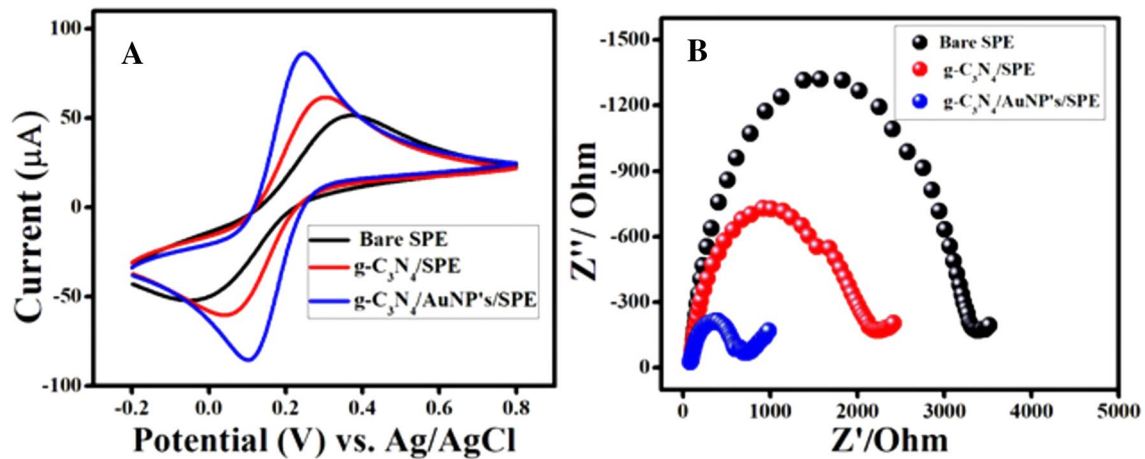


**Fig. 3** **A** Cyclic voltammetric response of different electrodes in 5 mM of  $[\text{Fe}(\text{CN})_6]^{3-/4-}$  in 0.1 M KCl as supporting electrolyte and **B** EIS response of different electrodes

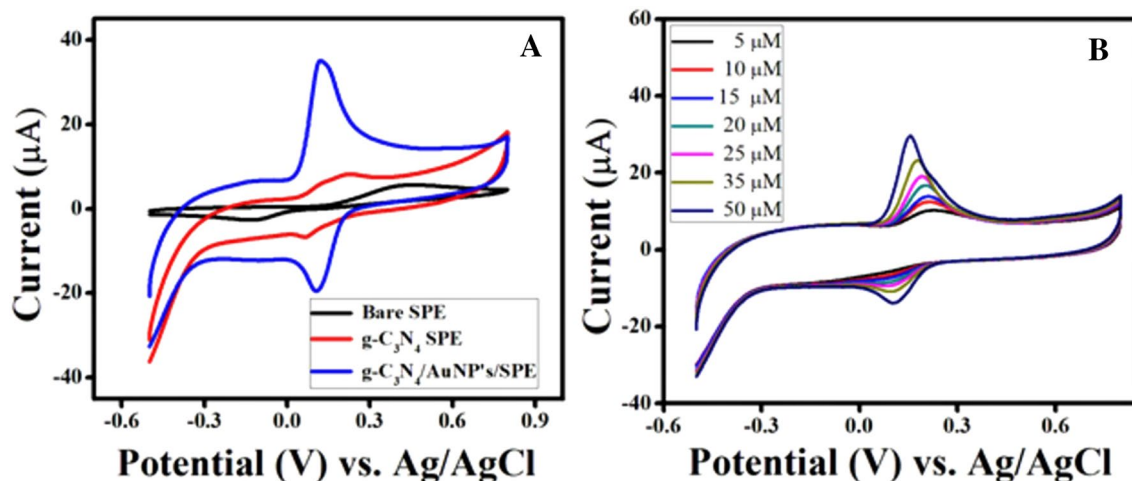


**Fig. 4** **A** Cyclic voltammetric response of different modified electrodes in 60  $\mu\text{M}$  of CA in 0.1 M PBS (pH 7) and **B** Cyclic voltammetric response of  $g\text{-C}_3\text{N}_4/\text{AuNPs}/\text{SPE}$  with different concentrations of CA in 0.1 M PBS pH-7.0 at a scan rate of  $50 \text{ mVs}^{-1}$

Then, 3  $\mu\text{L}$  of ultrathin  $\text{g-C}_3\text{N}_4/\text{AuNPs}$  nanocomposite was drop casted on SPE and dried under a nitrogen atmosphere at an ambient temperature. The as-prepared nanocomposite modified electrode ( $\text{g-C}_3\text{N}_4/\text{AuNPs}/\text{SPE}$ ) was evaluated towards electrochemical sensing of CA in different food samples.

## Results and discussion

### Structural characterization

The structural morphology of the synthesized bulk  $\text{g-C}_3\text{N}_4$  was investigated using FE-SEM analysis. FE-SEM image (Fig. 1a) shows a layered type of sheets-shaped  $\text{g-C}_3\text{N}_4$ . Further, ultrasonication-assisted acid-treated treated  $\text{g-C}_3\text{N}_4$  was prepared, and the morphology was investigated using TEM. Figure 1b shows the TEM image of ultrathin  $\text{g-C}_3\text{N}_4$ , which confirmed the thin nanosheet-like structure. Figure 1c indicates the spherical-shaped morphology of citrate-capped AuNPs. Figure 1d and e show the TEM images of the ultrathin  $\text{g-C}_3\text{N}_4/\text{AuNPs}$  composite that exhibited the uniform distribution/decoration of spherical-shaped AuNPs on the ultrathin  $\text{g-C}_3\text{N}_4$  nanosheets. Moreover, carbon, nitrogen, and AuNPs of the as-prepared nanocomposite were also confirmed with EDS analysis, and the results are shown in Fig. 1f.

Figure 2 illustrates the XRD pattern of the as-prepared bulk  $\text{g-C}_3\text{N}_4$  and ultrathin  $\text{g-C}_3\text{N}_4/\text{AuNPs}$  nanocomposite. The characteristic diffraction peak at  $2\theta$  of  $27.5^\circ$  corresponded to 002 planes of bulk  $\text{g-C}_3\text{N}_4$ , indicating the interlayer arrangements of aromatic rings of  $\text{g-C}_3\text{N}_4$  (Ramalingam et al. 2019). Two characteristic diffraction peaks were observed at  $38.2^\circ$  and  $44.3^\circ$ , corresponding to the Au (111, 200) planes (Lv 2018) of the AuNPs/ $\text{g-C}_3\text{N}_4$  nanosheets composite. Therefore, XRD results indicated that the AuNPs were successfully decorated on the ultrathin  $\text{g-C}_3\text{N}_4$  nanosheets.

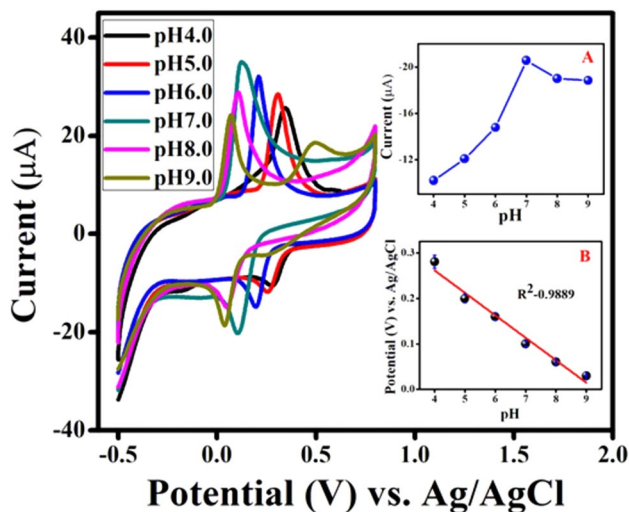


**Fig. 5** Cyclic voltammogram of 60  $\mu\text{M}$  of CA in different pH conditions in the range from 4.0 to 9.0 and the inset figure (a) relationship between pH vs.  $I_{pa}$  (b) pH vs.  $E_{pa}$

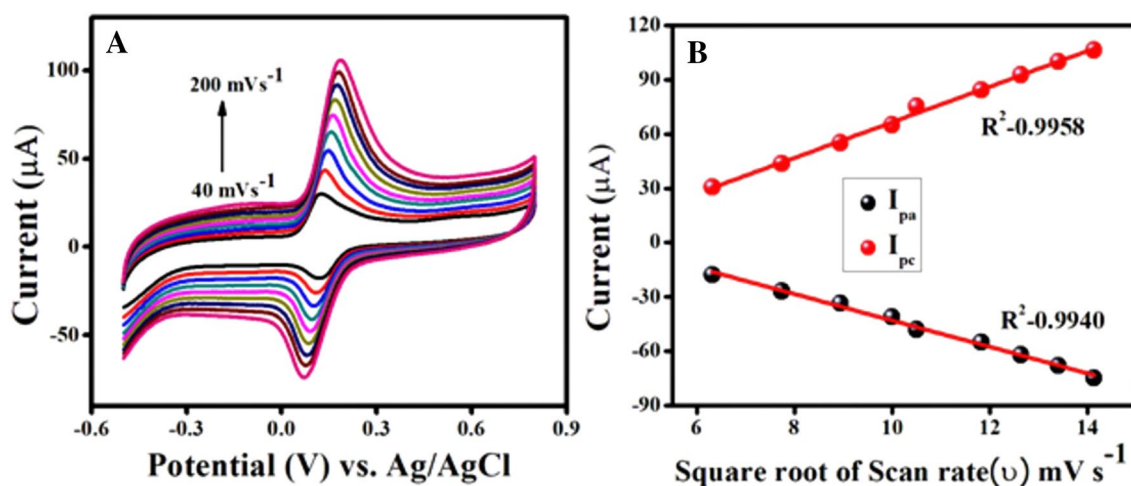


**Fig. 6** A Cyclic voltammogram of different scan rate from 40 to 200  $\text{mV s}^{-1}$  in the presence of 60  $\mu\text{M}$  of CA in 0.1 M PBS (pH 7) B Relationship between the square root of scan rate ( $v$ ) vs.  $I_{pa}$  and  $I_{pc}$

## Electrochemical study

The electrocatalytic nature of the as-prepared  $g\text{-C}_3\text{N}_4/\text{AuNPs}$  coated SPE sensor was evaluated using the cyclic voltammetry technique. Figure 3a indicates cyclic voltammograms recorded at 5 mM of  $[\text{Fe}(\text{CN})_6]^{3-/4-}$  containing 0.1 M KCl (as supporting electrolyte) solution. From the cyclic voltammetric behavior, it was observed that  $g\text{-C}_3\text{N}_4/\text{AuNPs}/\text{SPE}$  exhibited higher redox peak currents with lower potential values and the peak-to-peak separation ( $\Delta E_p$ ) of 0.13 mV. In contrast, the  $\Delta E_p$  of bare and  $g\text{-C}_3\text{N}_4$

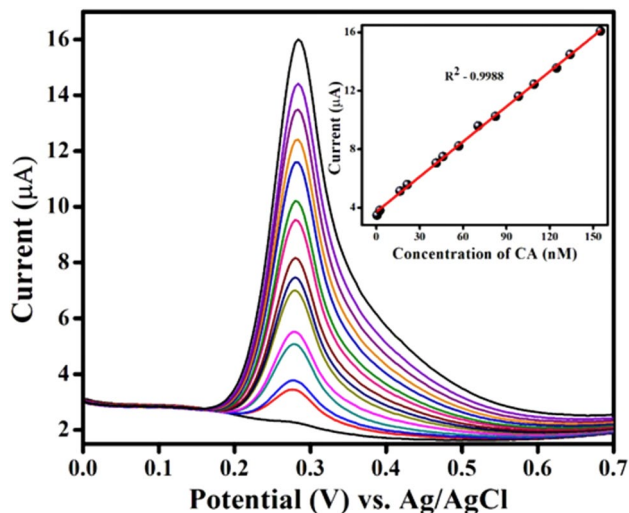


**Fig. 7** DPV response of different concentrations of CA in 0.1 M PBS (pH7) as supporting electrolyte and CA determination in the range from 0.5 to 155 nM and corresponding calibration plot

were found at 0.40 and 0.24 mV, respectively. The fast electron-transfer kinetics of  $[\text{Fe}(\text{CN})_6]^{3-/4-}$ , higher redox peak currents, and the lowest  $\Delta E_p$  of  $g\text{-C}_3\text{N}_4/\text{AuNPs}/\text{SPE}$  were used for further electrochemical experiments.

Electrochemical impedance spectroscopy (EIS) is an important technique to study the interfacial behavior between the electrolyte solution and the developed electrode surface. EIS analysis of bare SPE,  $g\text{-C}_3\text{N}_4/\text{SPE}$ , and  $g\text{-C}_3\text{N}_4/\text{AuNPs}/\text{SPE}$  was done in 5 mM of  $[\text{Fe}(\text{CN})_6]^{3-/4-}$  containing 0.1 M KCl supporting electrolyte with the applied frequencies ranging from 0.1 Hz to 100 kHz and the obtained Nyquist form of the results is shown in Fig. 3b. From the EIS data, the half-circular diameter was similar to the charge-transfer resistance ( $R_{ct}$ ) that belonged to the kinetics' behavior of electron transfer at the electrode surface/electrolyte interface (Hollaender 1997). The  $R_{ct}$  of the bare SPE,  $g\text{-C}_3\text{N}_4/\text{SPE}$ , and  $g\text{-C}_3\text{N}_4/\text{AuNPs}/\text{SPE}$  were 3358  $\Omega$ , 2155  $\Omega$ , and 672  $\Omega$ , respectively. The bulk  $g\text{-C}_3\text{N}_4$  showed a low value of  $R_{ct}$  when compared with the AuNPs decorated  $g\text{-C}_3\text{N}_4$  nanosheets composite. Thus, the obtained EIS results also ensured that the AuNPs were firmly attached to the ultrathin  $g\text{-C}_3\text{N}_4$  nanosheets.

## Electrocatalytic studies of $g\text{-C}_3\text{N}_4/\text{AuNPs}/\text{SPE}$ towards detection of CA

The fabricated  $g\text{-C}_3\text{N}_4/\text{AuNPs}/\text{SPE}$  sensor was applied to detect CA by the cyclic voltammetric method. Figure 4a shows the cyclic voltammetric response of 60  $\mu\text{M}$  of CA in 0.1 M phosphate buffer (PBS, pH 7.0) with modified electrodes. Bare SPE showed a very low anodic peak current ( $-3.01 \mu\text{A}$ ) and a higher anodic peak potential (0.16 V) due

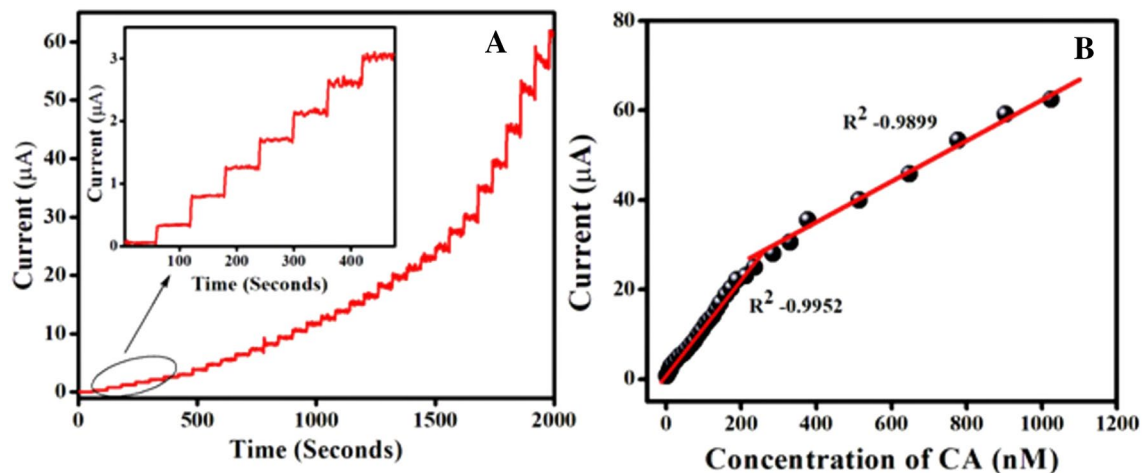


**Fig. 8** A Amperometric-t response of  $g\text{-C}_3\text{N}_4/\text{AuNPs}/\text{SPE}$  modified electrode with different concentrations of CA (2.5 to 1025 nM) in 0.1 M PBS pH-7.0 at an applied potential of 0.2 V and B The relationship between the concentration of CA and corresponding anodic peak current response

tionship between the concentration of CA and corresponding anodic peak current response

**Table 1** Analytical performance different modified electrode towards CA determination

Electrode	Linear range ( $\mu\text{M}$ )	LOD* ( $\mu\text{M}$ )	Sensitivity ( $\mu\text{M}/\mu\text{A}$ )	Technique	Ref
g-C <sub>3</sub> N <sub>4</sub> /AuNPs/SPE	0.0005–0.155 0.000025–1.025	0.0005	0.0001 152.24 138.02	DPV Amp	This work
HMGO <sup>a</sup> (800)/GCE	0.01–608	0.004	429.0	Amp	(Sivasankar et al. 2018)
Au/PdNPs/GRF <sup>b</sup> /GCE	0.03–938.97	0.006	NA	DPV	(Thangavelu et al. 2017)
Pt-PEDOT/rGO <sup>c</sup> /GCE	0.005–0.5	0.002	NA	DPV	(Gao 2018)
Au-PEDOT/rGO <sup>d</sup> /GCE	0.01–46	0.004	NA	DPV	(Liu 2016)
MnO <sub>2</sub> /CM <sup>e</sup> /GCE	0.01–1.0	0.002	4.638	SWV	(Li et al. 2017)
3DG/MWCNT <sup>f</sup> /GCE	0.2–174	0.017	NA	Amp	(Sakthnathan et al. 2017)
CoFeS <sub>2</sub> /GCE <sup>g</sup>	0.01–263.96	0.002	2.04	DPV	(Sakthivel et al. 2018)
AuNPs/G/GCE <sup>h</sup>	0.5–5.0	0.05	NA	DPV	(Zhang et al. 2013)
Au@ $\alpha$ -Fe <sub>2</sub> O <sub>3</sub> @rGO/ GCE <sup>i</sup>	19–1869	0.098	315	DPV	(Bharath et al. 2018)

Abbreviations: \*LOD limit of detection, Amp amperometry, SWV square wave voltammetry, GCE glassy carbon electrode, **a** hierarchical mesoporous graphite oxide/Al<sub>2</sub>O<sub>3</sub>, **b** gold/palladium nanoparticles on graphene flakes, **c** Pt-PEDOT/reduced graphene oxide, **d** Au-PEDOT/reduced graphene oxide, **e** MnO<sub>2</sub>-embedded hierarchical porous carbon microspheres, **f** Three dimensional graphene/MWCNTs composite, **g** bimetallic CoFeS<sub>2</sub>/carbon nanofiber, **h** gold nanoparticles/graphene nanosheets and **i** Au@  $\alpha$ -Fe<sub>2</sub>O<sub>3</sub>@reduced graphene oxide

to poor electron-transfer behavior. The g-C<sub>3</sub>N<sub>4</sub>/SPE indicated CA oxidation peak current at  $-6.67 \mu\text{A}$  at a potential of 0.14 V. The g-C<sub>3</sub>N<sub>4</sub>/AuNPs/SPE exhibited the highest peak current at  $-19.62 \mu\text{A}$  and the lowest potential of 0.10 V due to the g-C<sub>3</sub>N<sub>4</sub> nanosheets being decorated with AuNPs that helped the fast electron-transfer towards CA oxidation. Further, the g-C<sub>3</sub>N<sub>4</sub>/AuNPs/SPE sensor was examined at various CA concentrations in 0.1 M PBS (pH7.0) supporting electrolyte by adding various concentrations of CA from 5 to 50  $\mu\text{M}$  (Fig. 4b), indicating a linear increase in the anodic peak current without any surface poisoning effect.

### Effect of pH and scan rate towards detection of CA

The influence of the supporting electrolyte pH towards detecting 60  $\mu\text{M}$  of CA was investigated in different pH ranges from 4.0 to 9.0 using the g-C<sub>3</sub>N<sub>4</sub>/AuNPs/SPE sensor and the corresponding anodic peak potential, and the current response of the cyclic voltammograms is shown in Fig. 5. From the cyclic voltammetric response, while increasing the pH condition, the anodic peak potential of CA moved towards the negative direction (Thangavelu et al. 2017) exhibited the protons involved in the electrode reaction. However, increasing the pH stimulated the deprotonation of the CA oxidation process. Figure 5b indicates the anodic peak potentials of CA at various pH conditions. A linear regression equation of  $E_{pa} (\text{V}) = -0.158\text{pH} + 0.4596\text{V}$  with  $R^2$  value of 0.9889 was obtained from the linear plot with 0.579 mV/pH as the slope value. However, the highest anodic peak current has been achieved at pH 7.0 (PBS) (Fig. 5a). Therefore, pH 7.0 was selected as the supporting electrolyte for subsequent electrochemical studies.

The effects of the scan rate of g-C<sub>3</sub>N<sub>4</sub>/AuNPs/SPE were tested using cyclic voltammetry to understand the charge-transfer behavior of the as-prepared electrode towards the detection of CA in 0.1 M PBS (pH 7.0) at various scan rates, and the results are exhibited in Fig. 6a. The redox peak current of CA showed a gradual increase while increasing the scan rate from 40 to 200  $\text{mVs}^{-1}$ , and the redox peak potential was shifted towards the negative direction. However, the anodic peak current was correlated with the square root of scan rate (Fig. 6b), and the linear regression equation was  $I_{pa} (\mu\text{A}) = 29.9235(v) + 7.2857$  ( $R^2 = 0.9940$ ) and  $I_{pc} (\mu\text{A}) = 31.7166(v) + 9.8237$  ( $R^2 = 0.9958$ ) for anodic and cathodic peak currents, respectively. The obtained correlation coefficient ( $R^2$ ) value concluded that the entire electrochemical reaction of CA at g-C<sub>3</sub>N<sub>4</sub>/AuNPs/SPE was a diffusion-controlled process (Sakthnathan et al. 2017).

### Analytical performance

Differential pulse voltammetry (DPV) is a common electroanalytical method to study the different modified electrodes' electrochemical response compared with other cyclic voltammetric techniques. DPV technique is also a beneficial tool to estimate the analytical parameters, including linear range, detection limit, and sensitivity of the target analyte. Figure 7 indicates the DPV response of the as-prepared g-C<sub>3</sub>N<sub>4</sub>/AuNPs/SPE at various concentrations of CA from 0.5 to 155 nM (oxidation potential of 0.29 V) in 0.1 M PBS (pH 7.0) as the supporting electrolyte. The obtained anodic peak currents were plotted against the various concentrations of CA, and a linear regression equation ( $I_{pa} (\mu\text{A}) = 3.708x + 0.801y$ ) was obtained with the  $R^2$  value of 0.9988. The detection limit (LOD) was calculated by

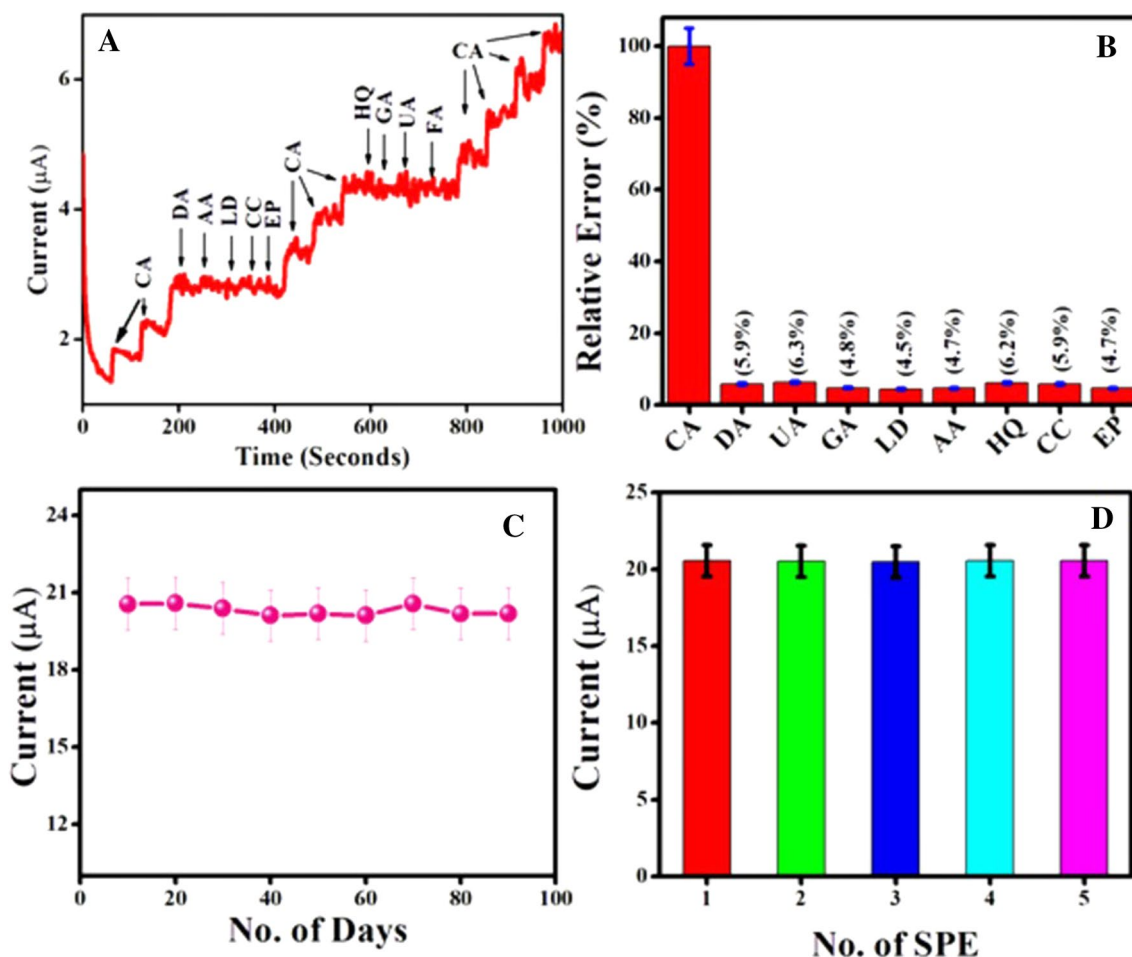


**Fig. 9** **A** amperometric *i-t* response of  $g\text{-C}_3\text{N}_4/\text{AuNPs}/\text{SPE}$  electrode at different concentration of CA in the presence of 50 fold excess of different interfering species, **B** Interference study error bar diagram, **C** Stability study of the modified electrode over 90 days in the pres-

ence of 50  $\mu\text{M}$  of CA in 0.1 M PBS (pH 7.0) and **D** Reproducibility test bar diagram of various  $g\text{-C}_3\text{N}_4/\text{AuNPs}/\text{SPE}$  modified electrode towards detection of 50  $\mu\text{M}$  CA in 0.1 M PBS pH-7.0

$3\sigma/S = \text{LOD}$  (where,  $\sigma$ - DPV response of blank signals of standard deviation and  $S$ -the slope value from the calibration equation) and the LOD of CA was 0.3 nM, and the sensitivity of  $152.24 \mu\text{A}/\mu\text{M cm}^{-2}$  has been found from the proposed method.

Further, the modified  $g\text{-C}_3\text{N}_4/\text{AuNPs}/\text{SPE}$  sensor was tested for the detection of CA under dynamic conditions using the amperometric (*i-t*) technique with 0.2 V as the applied potential and  $50 \text{ mV s}^{-1}$  as the scan rate. Figure 8a shows the amperograms; a stable and speedy electrocatalytic current response was obtained for each addition of CA, which indicated good electrocatalytic behavior of  $g\text{-C}_3\text{N}_4/\text{AuNPs}/\text{SPE}$ . The electrocatalytic current response was measured within 4 s during the addition of CA, and ~98% of the steady-state anodic current responses were observed. Figure 8b indicates the calibration plot of the relationship between the CA concentrations and their corresponding catalytic currents. The analytical

parameters, including linear range, detection limit, and sensitivity, were calculated from the calibration plot and excellent linearity was achieved in the concentration range from 2.5 nM to 1025 nM with the detection limit of 0.53 nM and sensitivity of  $138.02 \mu\text{A}/\mu\text{M cm}^{-2}$  for CA. The excellent electrocatalytic behavior of the developed  $g\text{-C}_3\text{N}_4/\text{AuNPs}/\text{SPE}$  sensor was achieved because of the high surface area of ultrathin  $g\text{-C}_3\text{N}_4$  nanosheets and the superior catalytic activity of AuNPs. Further, the analytical performance of the presented work was also compared with other previously reported analytical sensing methods of CA and are tabulated in Table 1.

### Interference studies

The fabricated  $g\text{-C}_3\text{N}_4/\text{AuNPs}/\text{SPE}$  was tested with various interferences using the amperometric *i-t* technique in the presence of 50 fold excess quantity of other electroactive



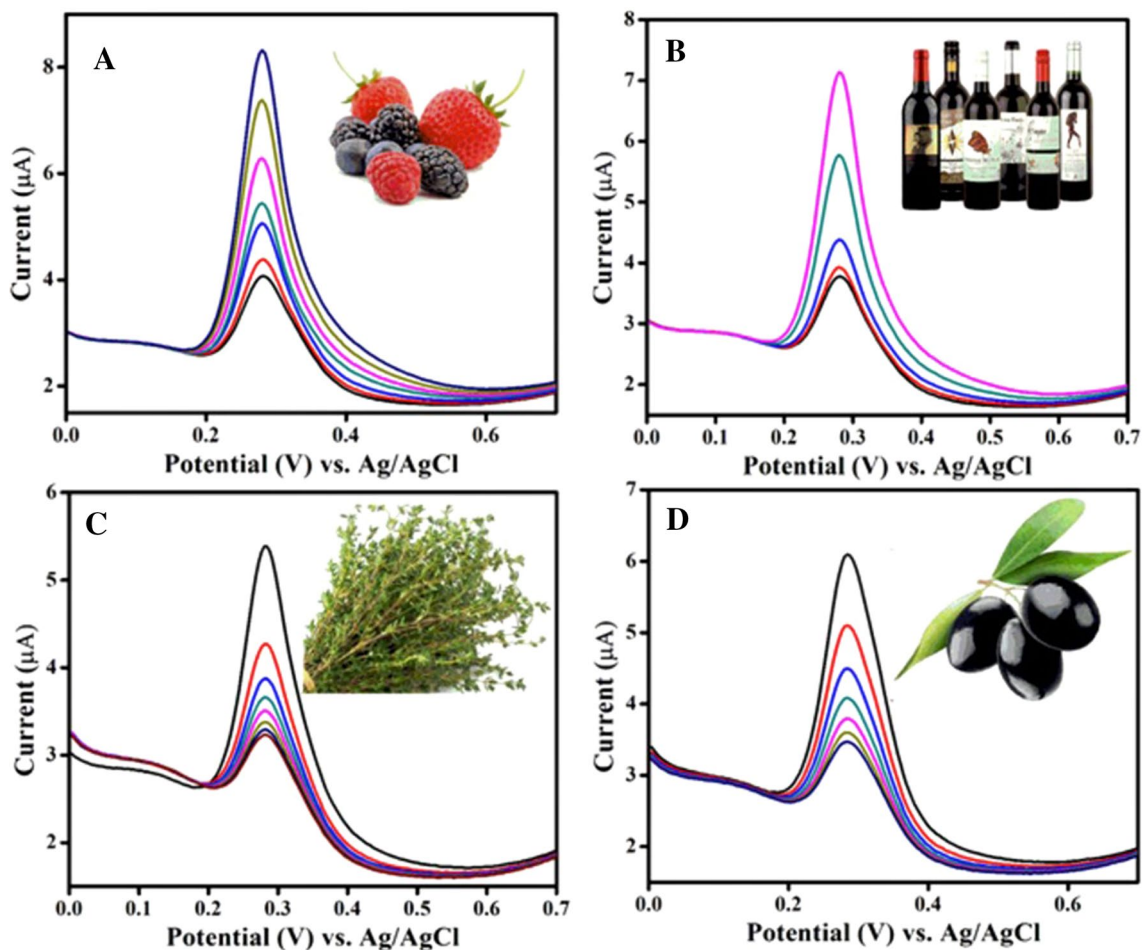


**Fig. 10** DPV response for the determination CA in different real samples **A** Strawberry fruit juice, **B** Red wine samples, **C** Thyme leaves and **D** black fruit juice samples

analytes, including uric acid (UA), gallic acid (GA), ascorbic acid (AA), catechol (CC), hydroquinone (HQ), epinephrine (EP), folic acid (FA), L-dopa (LD) and dopamine (DA) and the experimental data are exhibited in Fig. 9a. All the abovementioned analytes have not interfered, and the anodic peak current of CA did not show any apparent changes, and only about <7% of anodic peak current variation of CA was measured because of the addition of different interfering species, the corresponding standard error bar diagram was plotted, and the results are shown in Fig. 9b. The g-C<sub>3</sub>N<sub>4</sub> nanosheets decorated AuNPs nanocomposite showed excellent electrocatalytic behavior in the electrochemical oxidation and detection of CA due to the adsorption of CA on the g-C<sub>3</sub>N<sub>4</sub>/AuNPs/SPE surface that facilitated higher charge-transfer for the CA oxidation process. Moreover, the formation of hydrogen bonding interaction between the carboxylic acid functional group present in CA and aromatic triazine in the g-C<sub>3</sub>N<sub>4</sub> also increased the charge-transfer reaction. Therefore, the general interfering analyte species were not involved in the electrocatalytic oxidation of CA

even at higher concentrations in sample matrices. Hence, the developed g-C<sub>3</sub>N<sub>4</sub>/AuNPs/SPE sensor was highly selective towards the sensing of CA.

### Stability and reproducibility

Studying the stability of the g-C<sub>3</sub>N<sub>4</sub>/AuNPs/SPE is vital to evaluate the sensor's performance. The stability of the proposed sensor was tested by performing over 90 days using the cyclic voltammetry technique in the presence of 50 μM of CA in 0.1 M PBS (pH 7.0) with a scan rate of 50 mV s<sup>-1</sup>, and the obtained results are exhibited in Fig. 9c. The g-C<sub>3</sub>N<sub>4</sub>/AuNPs/SPE has shown high, long-term stability towards the detection of CA. Further, the reproducibility of the modified electrodes was tested by using five different g-C<sub>3</sub>N<sub>4</sub>/AuNPs/SPE and the corresponding cyclic voltammetric current values are shown in Fig. 9d. From the reproducibility results, the relative standard deviation (RSD) was calculated, and the RSD

**Table 2** Determination of CA in different food samples using g-C<sub>3</sub>N<sub>4</sub>/AuNPs/SPE

Sample name	Added (nM)	Found (nM)	RSD (% , n=3)	Recovery (%)
Strawberry fruit	5	4.9 (±0.3)	1.3	98
	10	10.03 (±0.04)	1.7	100.3
	20	20.01 (±0.13)	1.9	100.05
	30	29.91 (±0.11)	2.1	99.7
	40	40.01 (±0.71)	1.3	100.02
Red wine	5	5.03 (±0.07)	1.4	100.6
	10	9.99 (±0.17)	1.1	99.9
	20	20.07 (±0.08)	1.8	100.3
	30	29.7 (±0.13)	1.9	99
	40	40.13 (±0.17)	1.3	100.3
White wine	5	4.93 (±0.04)	1.3	98.6
	10	10.07 (±0.13)	1.7	100.7
	20	20.13 (±0.07)	1.9	100.65
	30	29.9 (±0.03)	1.6	99.6
	40	40.1 (±0.03)	1.9	100.25
Thyme leaves	5	5.03 (±0.06)	1.9	100.6
	10	9.99 (±0.02)	1.6	99.9
	20	20.07 (±0.37)	1.5	100.3
	30	30.07 (±0.03)	1.4	100.2
	40	40.13 (±0.04)	1.9	100.3
Black fruit	5	5.03 (±0.01)	1.9	100.6
	10	10.04 (±0.02)	2.1	100.4
	20	20.07 (±0.31)	2	100.3
	30	30.07 (±0.17)	1.8	100.2
	40	40.10 (±0.03)	1.7	100.2

was 2.3%. Hence, the g-C<sub>3</sub>N<sub>4</sub>/AuNPs/SPE exhibited good reproducibility towards the detection of CA.

### Practical applicability of the g-C<sub>3</sub>N<sub>4</sub>/AuNPs/SPE sensor

To study the practical ability of the proposed ultrathin g-C<sub>3</sub>N<sub>4</sub>/AuNPs/SPE sensor, the developed electrode was applied to estimate CA in various real samples (food and wine samples) using the DPV technique under optimized experimental conditions. 20 mL of freshly prepared strawberry fruit juice, thyme leaf juice, black fruit juice, and red wine samples were chosen as real samples to determine the CA. 50 mL of fresh juice samples was taken and diluted to 250 mL using the buffer solution (PBS, pH 7.0). 50 mL of the spiked buffered sample solution (5 mM of standard CA solution was used for spiking) was taken for the electrochemical analysis using the standard addition method under the DPV technique. The corresponding DPV response is shown in Fig. 10. The analytical parameter results such as recovery range, RSD values are tabulated and displayed in Table 2. The proposed method for CA analysis was attested

with excellent results compared with the earlier reported analytical methods. The average recovery range was found from 98.0% to 100.65% and the RSD was < 3%. Hence, the proposed g-C<sub>3</sub>N<sub>4</sub>/AuNPs/SPE would be a suitable sensing material for the practical utility of CA detection.

### Conclusion

AuNPs decorated ultrathin g-C<sub>3</sub>N<sub>4</sub> nanosheet composite material was successfully prepared via a simple sonochemical method. The developed ultrathin g-C<sub>3</sub>N<sub>4</sub>/AuNPs/SPE sensor showed an excellent electrochemical behavior towards detecting CA at the neutral pH environment (PBS, pH 7.0). The developed sensor showed excellent electrochemical current signals (lower oxidation potential with higher anodic peak current) with high stability and indicated high suitability for practical application towards the determination of CA in real samples. The g-C<sub>3</sub>N<sub>4</sub>/AuNPs/SPE sensor was successfully applied in various food samples to quantify CA, and the achieved results were satisfactory and promising over conventional and recently reported methods. Hence, the proposed sensor can be

utilized in routine food analysis and food quality control laboratories for quick, selective, and sensitive quantification of CA in foods.

**Acknowledgements** This research work was supported financially by the grant MOST107-2113-M-037-007-MY2 and MOST110-2113-M-037-009- from Ministry of Science and Technology (MOST), Taiwan, and also supported by the Research Center for Environmental Medicine, Kaohsiung Medical University, Kaohsiung, Taiwan from “The Featured Areas Research Center Program within the framework of the Higher Education Sprout Project” by the Ministry of Education (MOE) in Taiwan. The authors gratefully acknowledge the use of TEM, SEM, XRD, and XPS equipment provided by the Instrument Center of National Cheng Kung University, Tainan, Taiwan.

## Declarations

**Conflict of interest** The author(s) declare that they have no competing interests.

## References

- Cheng Y, He L, Xia G et al (2019) Nanostructured  $gC_3N_4/AgI$  composites assembled by AgI nanoparticles-decorated  $gC_3N_4$  nanosheets for effective and mild photooxidation reaction. *New J Chem* 43:14841–14852
- Dai G, Xie J, Li C, Liu S (2017) Flower-like  $Co_3O_4/graphitic$  carbon nitride nanocomposite based electrochemical sensor and its highly sensitive electrocatalysis of hydrazine. *J Alloys Compd* 727:43–51
- Ding M, Guo Z, Zhou L et al (2018) One-dimensional zinc oxide nanomaterials for application in high-performance advanced optoelectronic devices. *Curr Comput Aided Drug Des* 8:223
- Fan D, Jia L, Xiang H et al (2017) Synthesis and characterization of hollow porous molecular imprinted polymers for the selective extraction and determination of caffeic acid in fruit samples. *Food Chem* 224:32–36
- Gao L, Yue R, Xu J et al (2018) Pt-PEDOT/rGO nanocomposites: One-pot preparation and superior electrochemical sensing performance for caffeic acid in tea. *J Electroanal Chem* 816:14–20
- Ghafuri H, Jafari G, Rashidzadeh A, Manteghi F (2019)  $Co^{2+}$  immobilized on highly ordered mesoporous graphitic carbon nitride ( $omp-g-C_3N_4/Co^{2+}$ ) as an efficient and recyclable heterogeneous catalyst for one-pot tandem selective photo-oxidation/Knoevenagel condensation. *Mol Catal* 475:110491
- Han E-X, Li Y-Y, Wang Q-H et al (2019a) Chlorine doped graphitic carbon nitride nanorings as an efficient photoresponsive catalyst for water oxidation and organic decomposition. *J Mater Sci Technol* 35:2288–2296
- Han Y, Liu Y, Su C et al (2019) Interface engineered  $WS_2/ZnS$  heterostructures for sensitive and reversible  $NO_2$  room temperature sensing. *Sensors Actuators B Chem* 296:126666
- Hollaender J (1997) Rapid assessment of food/package interactions by electrochemical impedance spectroscopy (EIS). *Food Addit Contam* 14:617–626
- Karthick Kannan P, Shankar P, Blackman C, Chung C-H (2019) Recent advances in 2D inorganic nanomaterials for SERS sensing. *Adv Mater* 31:1803432
- Lee H, Yoon SW, Kim EJ, Park J (2007) In-situ growth of copper sulfide nanocrystals on multiwalled carbon nanotubes and their application as novel solar cell and amperometric glucose sensor materials. *Nano Lett* 7:778–784
- Leite FRF, de Santos W, JR, Kubota LT, (2014) Selective determination of caffeic acid in wines with electrochemical sensor based on molecularly imprinted siloxanes. *Sensors Actuators B Chem* 193:238–246
- Li J, Jiang J, Liu M et al (2017) Facile synthesis of  $MnO_2$ -embedded flower-like hierarchical porous carbon microspheres as an enhanced electrocatalyst for sensitive detection of caffeic acid. *Anal Chim Acta* 985:155–165
- Li Y, Peng Y-K, Hu L et al (2019) Photocatalytic water splitting by N-TiO<sub>2</sub> on MgO (111) with exceptional quantum efficiencies at elevated temperatures. *Nat Commun* 10:1–9
- Liu L, Wang J, Wang C, Wang G (2016a) Facile synthesis of graphitic carbon nitride/nanostructured  $g-C_3N_4-Fe_2O_3$  composites and their excellent electrochemical performance for supercapacitor and enzyme-free glucose detection applications. *Appl Surf Sci* 390:303–310
- Liu Z, Xu J, Yue R et al (2016b) Facile one-pot synthesis of Au-PEDOT/rGO nanocomposite for highly sensitive detection of caffeic acid in red wine sample. *Electrochim Acta* 196:1–12
- Lu Q, Deng J, Hou Y et al (2015) One-step electrochemical synthesis of ultrathin graphitic carbon nitride nanosheets and their application to the detection of uric acid. *Chem Commun* 51:12251–12253
- Luo B, Song R, Geng J et al (2019) Towards the prominent cocatalytic effect of ultra-small CoP particles anchored on  $g-C_3N_4$  nanosheets for visible light driven photocatalytic  $H_2$  production. *Appl Catal B Environ* 256:117819
- Lv S, Sheng J, Zhao S et al (2018) The detection of brucellosis antibody in whole serum based on the low-fouling electrochemical immunosensor fabricated with magnetic  $Fe_3O_4@Au@PEG@HA$  nanoparticles. *Biosens Bioelectron* 117:138–144
- Prabhu P, Babu RS, Narayanan SS (2011) Amperometric determination of l-dopa by nickel hexacyanoferrate film modified gold nanoparticle graphite composite electrode. *Sensors Actuators B Chem* 156:606–614
- Prasad NR, Jeyanthimala K, Ramachandran S (2009) Caffeic acid modulates ultraviolet radiation-B induced oxidative damage in human blood lymphocytes. *J Photochem Photobiol B Biol* 95:196–203
- Ramalingam M, Ponnusamy VK, Sangilimuthu SN (2019) A nanocomposite consisting of porous graphitic carbon nitride nanosheets and oxidized multiwalled carbon nanotubes for simultaneous stripping voltammetric determination of cadmium (II), mercury (II), lead (II) and zinc (II). *Microchim Acta* 186:1–10
- Safaei J, Mohamed NA, Noh MFM et al (2018a) Graphitic carbon nitride ( $gC_3N_4$ ) electrodes for energy conversion and storage: a review on photoelectrochemical water splitting, solar cells and supercapacitors. *J Mater Chem A* 6:22346–22380
- Safaei J, Ullah H, Mohamed NA et al (2018b) Enhanced photoelectrochemical performance of Z-scheme  $g-C_3N_4/BiVO_4$  photocatalyst. *Appl Catal B Environ* 234:296–310
- Sakthianathan S, Kubendhiran S, Chen S-M (2017) Hydrothermal synthesis of three dimensional graphene-multiwalled carbon nanotube nanocomposite for enhanced electro catalytic oxidation of caffeic acid. *Electroanalysis* 29:1103–1112
- Sakthivel M, Ramaraj S, Chen S-M et al (2018) Entrapment of bimetallic  $CoFeSe_2$  nanosphere on functionalized carbon nanofiber for selective and sensitive electrochemical detection of caffeic acid in wine samples. *Anal Chim Acta* 1006:22–32
- Samanta S, Yadav R, Kumar A et al (2019) Surface modified C, O co-doped polymeric  $g-C_3N_4$  as an efficient photocatalyst for visible light assisted  $CO_2$  reduction and  $H_2O_2$  production. *Appl Catal B Environ* 259:118054
- Shrestha BK, Ahmad R, Shrestha S et al (2017) In situ synthesis of cylindrical spongy polypyrrole doped protonated graphitic carbon nitride for cholesterol sensing application. *Biosens Bioelectron* 94:686–693

- Sikarwar S, Yadav BC (2015) Opto-electronic humidity sensor: A review. *Sensors Actuators A Phys* 233:54–70
- Sivasankar K, Devasenathipathy R, Wang S-F et al (2018) Synthesis of hierarchical mesoporous graphite oxide/ $\text{Al}_2\text{O}_3$  from MIL-100 (Al) for the electrochemical determination of caffeic acid in red wine samples. *J Taiwan Inst Chem Eng* 84:188–195
- Thangavelu K, Raja N, Chen S-M, Liao W-C (2017) Nanomolar electrochemical detection of caffeic acid in fortified wine samples based on gold/palladium nanoparticles decorated graphene flakes. *J Colloid Interface Sci* 501:77–85
- Tian H, Fan H, Ma J et al (2017) Noble metal-free modified electrode of exfoliated graphitic carbon nitride/ZnO nanosheets for highly efficient hydrogen peroxide sensing. *Electrochim Acta* 247:787–794
- Wang H, Provan GJ, Helliwell K (2004) Determination of rosmarinic acid and caffeic acid in aromatic herbs by HPLC. *Food Chem* 87:307–311
- Wang C, Li J, Luo X et al (2016) Graphitic carbon nitride nanosheets modified multi-walled carbon nanotubes as 3D high efficient sensor for simultaneous determination of dopamine, uric acid and tryptophan. *J Electroanal Chem* 780:147–152
- Zhang Y, Liu Y, He J et al (2013) Electrochemical behavior of caffeic acid assayed with gold nanoparticles/graphene nanosheets modified glassy carbon electrode. *Electroanalysis* 25:1230–1236
- Zhang S, Xie M, Li F et al (2016) Semiconducting group 15 monolayers: a broad range of band gaps and high carrier mobilities. *Angew Chemie* 128:1698–1701
- Zhang X, Shakeel M, Li B et al (2019) Fabrication of 3-D ZnO/CN nanorods for photo-/electrocatalytic water splitting: An efficient morphology for charge carriers transportation. *Int J Hydrogen Energy* 44:21821–21836
- Zhao Q, Wu W, Wei X et al (2017) Graphitic carbon nitride as electrode sensing material for tetrabromobisphenol-A determination. *Sensors Actuators B Chem* 248:673–681
- Zhao X, Pan D, Chen X et al (2019) g- $\text{C}_3\text{N}_s$  photoanode for photo-electrocatalytic synergistic pollutant degradation and hydrogen evolution. *Appl Surf Sci* 467:658–665

**Publisher's Note** Springer Nature remains neutral with regard to jurisdictional claims in published maps and institutional affiliations.